Experimental bounds on sterile neutrino mixing angles

Ruchayskiy, O.; Ivashko, A.

Experimental bounds on sterile neutrino mixing angles

Oleg Ruchayskiy[*] and Artem Ivashko[†‡]

Abstract

We derive bounds on the mixing between the Standard Model ("active") neutrinos and their right-chiral ("sterile") counterparts in the see-saw models, by combining neutrino oscillation data and results of direct experimental searches. We demonstrate that the mixing of sterile neutrinos with any active flavour can be significantly suppressed for the values of the angle θ_{13} measured recently by Daya Bay and RENO experiments. We reinterpret the results of searches for sterile neutrinos by the PS191 and CHARM experiments, considering not only charged current but also neutral current-mediated decays, as applicable in the case of see-saw models. The resulting *lower bounds* on sterile neutrino lifetime are up to an order of magnitude *stronger* than previously discussed in the literature. Combination of these results with the upper bound on the lifetime coming from primordial nucleosynthesis rule out the possibility that two sterile neutrinos with the masses between 10 MeV and the pion mass are solely responsible for neutrino flavour oscillations. We discuss the implications of our results for the Neutrino Minimal Standard Model (the νMSM).

1 Introduction

Transitions between neutrinos of different flavours (see e.g. [1] for a review and Refs. [2–4] for the recent update of experimental values) are among the few firmly established phenomena *beyond the Standard Model of elementary particles*. The simplest explanation is provided by the "neutrino flavour oscillations" – non-diagonal matrix of neutrino propagation eigenstates in the weak charge basis. While the absolute scale of neutrino masses is not established, particle physics measurements put the sum of their masses below 2 eV [5] while from the cosmological data one can infer an upper bound of 0.58 eV at 95% CL [6].

A traditional explanation of the smallness of neutrino masses is provided by the *see-saw mechanism* [7–10]. It assumes the existence of several *right-handed neutrinos*, coupled to their Standard Model (SM) counterparts via the Yukawa interaction, providing the Dirac masses, $M_{\rm D}$, for neutrinos. The Yukawa interaction terms dictate the SM charges of the right-handed particles: they turn out to carry no electric, weak and strong charges; therefore they are often termed "singlet," or "sterile" fermions. Sterile neutrinos can thus have Majorana masses, M_s,

---

[*]CERN Physics Department, Theory Division, CH-1211 Geneva 23, Switzerland

[†]Instituut-Lorentz for Theoretical Physics, Universiteit Leiden, Niels Bohrweg 2, Leiden, The Netherlands

[‡]Department of Physics, Kiev National Taras Shevchenko University, Glushkov str. 2 building 6, Kiev, 03022, Ukraine

consistent with the gauge symmetries of the Standard Model. If the Majorana masses are much larger than the Dirac ones, the *type I seesaw formula* [7–10] holds, expressing the mass matrix of observed neutrinos ($\mathcal{M}_\nu$) via

$$\mathcal{M}_\nu = -M_{\mathrm{D}} M_s^{-1} M_{\mathrm{D}}^T, \tag{1}$$

where $\mathcal{M}_\nu$ is a 3×3 matrix of active neutrino masses, mixings, and (possible) CP-violating phases. The masses of sterile neutrinos are given by the eigenvalues of their Majorana mass matrix (with the corrections of the order M_{D}^2/M_s^2). They are much heavier than the active neutrino masses as a consequence of (1).

Numerous searches for sterile neutrinos in the mass range up to ~ 100 GeV had been performed (see the corresponding section in Particle Data Group [5],[1] see also [11] and refs. therein). These searches provided upper bounds on the strength of interaction of these neutral leptons with the SM neutrinos of different flavours – active-sterile neutrino *mixing angles* $\vartheta_\alpha^2 \propto \left| \frac{M_{\mathrm{D},\alpha}}{M_s} \right|^2$ for sterile neutrino with the mass M_s.[2] These bounds then can be interpreted as *lower bounds* on the lifetime of sterile neutrinos τ_s via

$$\tau_s^{-1} = \frac{G_F^2 M_s^5}{96\pi^3} \sum_X \vartheta_\alpha^2 B_X^{(\alpha)}, \tag{2}$$

where the sum runs over various particles to which sterile neutrino can decay, depending on their mass (ν, $e^\pm$, $\mu^\pm$, $\tau^\pm$, π, K, heavier mesons and baryons) and dimensionless quantities B_X^α depend on the branching ratios (see Appendix A for details). The lower bound on the lifetime τ_s is usually dominated by the least constrained mixing angle, ϑ_τ^2 (as will be shown later).

This bound can be made *stronger* if one assumes that the same particles are also responsible for the neutrino oscillations. The see-saw formula (1) limits (at least partially) possible values of ratios of the mixing angles $\vartheta_\alpha^2/\vartheta_\beta^2$. In the simplest case when only two sterile neutrinos are present (the minimal number, required to explain two observed neutrino mass differences) the ratios of mixing angles varies within a limited range, see e.g. [12, 13]. While this range can be several orders of magnitude large (owing to our ignorance of certain oscillation parameters, such as e.g. a CP-violating phase [12, 13]), the implied (lower) bounds on the lifetime become much stronger, essentially being determined by the *strongest*, rather than the weakest direct bound on ϑ_α. When confronted with the upper bound from Big Bang Nucleosynthesis [14, 15], they seem to close the window of parameters for sterile neutrinos with the mass lighter than about 150 MeV [12, 16]. It was argued in [17], however, that in the case of normal hierarchy there can be a small allowed window of parameters of sterile neutrinos with the mass below the pion mass.

In this paper we reanalyze restrictions on sterile neutrino lifetime in view of the recent results of the Daya Bay [18] and RENO [19] collaborations, that measured a non-zero mixing angle θ_{13} (see also [20, 21]). We demonstrate that in the case when there are only two sterile neutrinos, responsible for the observed neutrino oscillations, the oscillation data allow for such a choice of the active-sterile Yukawa couplings that the mixing of sterile neutrinos with any

---

[1] http://pdglive.lbl.gov/Rsummary.brl?nodein=S077&inscript=Y

[2] Here and below we use the letter ϑ for *active-sterile mixing angles* (defined by Eq. (11) below) while reserving θ_{12}, θ_{13} and θ_{23} for the measured parameters of the active neutrinos matrix $\mathcal{M}_\nu$. These quantities ϑ_α are often denoted $|V_{4\alpha}|^2$ or $|U_{x\alpha}|^2$ in the experimental papers, to which we refer. Here and below the Greek letters α, β are flavour index e, μ, τ and $i, j = 1, 2, 3$ denote active neutrino mass eigenstates.

given flavour can be strongly suppressed. This happens *only* for a non-zero values of θ_{13}, in the range consistent with the current measurements [2, 4, 18, 19]. We also confront our results with the recently reanalyzed bounds from primordial nucleosynthesis [22] and show that the window in the parameter space of sterile neutrinos with masses $10\,\mathrm{MeV} \lesssim M_s \lesssim 140\,\mathrm{MeV}$ discussed in previous works [17] (see also [12]) is closed. For larger masses the window remains open. The results of this paper partially overlap with [17] (also [23]), and we compare in the corresponding places to the previous works.

The paper is organized as follows: in Section 2 we briefly describe the type I see-saw model we use. We then investigate the relations between different mixing angles imposed by the see-saw mechanism and demonstrate that the mixing with any flavour ϑ_α^2 can become suppressed (Section 3). Section 4 is devoted to the overview of the experiments, searching for sterile neutrinos with the masses below $2\,\mathrm{GeV}$, and the way one should interpret their results to apply to the see-saw models that we study. Section 5 summarizes our revised bounds on mixing angles and translates them into the resulting constraints on sterile neutrino lifetime (Figs. 7). We conclude in Section 6, discussing implications of our results and confronting them with the bounds from primordial nucleosynthesis.

2   Sterile neutrino Lagrangian

The minimal way to add sterile neutrinos to the Standard Model is provided by the Type I see-saw model [7–10] (see also [24–27] and refs. therein):

$$\Delta\mathcal{L}_N = \sum_{I,J=1}^{\mathcal{N}} i\bar{N}_I \partial_\mu \gamma^\mu N_I - \left(F_{\alpha I}\, \bar{L}_\alpha N_I \tilde{\Phi} - \frac{(M_s)_{IJ}}{2}\, \bar{N}_I^c N_J + h.c. \right) , \qquad (3)$$

where $F_{\alpha I}$ are new Yukawa couplings, Φ_i is the SM Higgs doublet, $\tilde{\Phi}_i = \epsilon_{ij}\Phi_j^\dagger$. This model is renormalizable, has the same gauge symmetries as the Standard Model, and contains $\mathcal{N}$ additional Weyl fermions N_I — sterile neutrinos (N_I^c being the charge-conjugate fermion, in the chiral representation of Dirac γ-matrices $N_I^c = i\gamma^2 N_I^\dagger$). The number of these singlet fermions must be $\mathcal{N} \geq 2$ to explain the data on neutrino oscillations. In the case of $\mathcal{N} = 2$ there are *11 new parameters* in the Lagrangian (3), while the neutrino mass/mixing matrix $\mathcal{M}_\nu$ has 7 parameters in this case. The situation is even more relaxed for $\mathcal{N} > 2$. The see-saw formula (1) does not allow to fix the scale of Majorana and Dirac $M_{\mathrm{D},\alpha I} = F_{\alpha I}\langle\Phi\rangle$ masses. In this work we will mostly concentrate on sterile neutrinos with their masses M_s in the MeV–GeV range – the range that is probed by the direct searches. To further simplify our analysis we will concentrate on the case when the masses of both sterile neutrinos are close to each other (so that $\Delta M \ll M_s$). One important example of such model is provided by the *Neutrino Extended Standard Model* (the νMSM) ([28, 29], see [16] for review). The νMSM model contains 3 sterile neutrinos, whose masses are roughly of the order of those of other leptons in the Standard Model. Two of these particles (approximately degenerate in their mass) are responsible for baryogenesis and neutrino oscillations and the third one is playing the role of dark matter. The requirement of dark matter stability on cosmological timescales makes its coupling with the Standard Model species so feeble, that it does not contribute significantly to the neutrino oscillation pattern [30]. Therefore, when analyzing neutrino oscillations, the N_1 can be omitted from the Lagrangian and index I in the sums

runs through 2 and 3 only:

$$\mathcal{L}_{see-saw} = \mathcal{L}_{SM} + \bar{N}_I i \partial_\mu \gamma^\mu N_I - M_{D,\alpha I} \bar{\nu}_\alpha N_I - M_{D,\alpha I}^* \bar{N}_I \nu_\alpha - M_s \bar{N}_2^c N_3 - M_s \bar{N}_3 N_2^c \ . \quad (4)$$

This parametrization coincides with [13, Eq. (2.1)]. Note that we use basis of singlet neutrinos where the mass matrix is off-diagonal. Recent computation of the baryon asymmetry of the Universe in the νMSM [31] demonstrated that sterile neutrinos with the mass as low as several MeV can be responsible for baryogenesis and neutrino oscillations within the νMSM. This prompts us to re-analyze the implication of negative direct experimental searches for the Yukawa couplings of sterile neutrinos with the MeV masses. We limit our analysis by $M_s \leq 2$ GeV, as for the higher masses the existing experimental bounds do not probe the region of mixing angles, required to produce successful baryogenesis in the νMSM [31].

3 Solution of the see-saw equations

In this Section we investigate how mixing angles between active and sterile neutrinos are related to parameters of the observable neutrino matrix $\mathcal{M}_\nu$. We will demonstrate that the mixing angle ϑ_e^2 in the case of normal hierarchy and the mixing angles ϑ_μ^2 or ϑ_τ^2 in the case of inverted hierarchy, can become suppressed as we vary the parameters of the neutrino matrix away from their best-fit values (but within the experimentally allowed 3σ bounds).

3.1 Parametrization of the Dirac mass matrix

We use the Pontecorvo–Maki–Nakagawa–Sakata (PMNS) parametrization of the neutrino matrix $\mathcal{M}_\nu$ (see e.g. Eqs.(2.10) and (2.12) of [1])

$$\mathcal{M}_\nu = V^* \, \text{diag}(m_1 e^{-2i\zeta}, \ m_2 e^{-2i\xi}, \ m_3) V^\dagger \ , \quad (5)$$

where V is the unitary matrix, whose explicit form is reminded in Appendix B. Redefining a Dirac mass matrix as[3]

$$M_D \to \tilde{M}_D \equiv V^T M_D \ , \quad (6)$$

we can rewrite the see-saw relation (1) in the following form:

$$\text{diag}(m_1 e^{-2i\zeta}, \ m_2 e^{-2i\xi}, \ m_3)_{ij} = -\frac{\tilde{M}_{D,i2}\tilde{M}_{D,j3} + \tilde{M}_{D,i3}\tilde{M}_{D,j2}}{M_s} \ , \quad (7)$$

The rank of the active neutrino mass matrix $\mathcal{M}_\nu$ is 2 in the case of two sterile neutrinos, meaning that one of the masses m_i is zero. Two choices of "hierarchies" of the mass eigenvalues are possible. The first one is called *normal hierarchy* (NH) and corresponds to $0 \leq m_1 < m_2 < m_3$. The second one is called *inverted hierarchy* (IH) and is realized for $0 \leq m_3 < m_1 < m_2$.

Once the mass M_s is fixed, the solutions of Eq. (7) contain one unknown complex parameter, z. Its presence reflects a symmetry of the see-saw relation (7) under the change $(\tilde{M}_{D,i2}, \tilde{M}_{D,i3}) \to (z\tilde{M}_{D,i2}, z^{-1}\tilde{M}_{D,i3})$ [32]. It is this freedom that does not allow to fix the absolute scale of $\tilde{M}_D$ (i.e. the value of ϑ^2) even if M_s is chosen.

The change $z \to z^{-1}$ is equivalent to the redefinition of $N_2 \to N_3$, $N_3 \to N_2$ together with shift of the Majorana phase $\xi \to \xi + \pi$ in (7). Therefore in subsequent analysis we will choose $|z| \geq 1$ without the loss of generality.

---

[3]The Dirac matrix $\tilde{M}_D$ has indexes $I = 2, 3$ and $i, j = 1, 2, 3$ – neutrino propagation basis

	Normal hierarchy	Inverted hierarchy
Δm_{21}^2	$(7.09 - 8.19) \times 10^{-5}$ eV^2	
Δm_{31}^2	$(2.14 - 2.76) \times 10^{-3}$ eV^2	Δm_{13}^2 $(2.13 - 2.67) \times 10^{-3}$ eV^2
$\sin^2 \theta_{12}$	$0.27 - 0.36$	
$\sin^2 \theta_{23}$	$0.39 - 0.64$	
$\sin^2 \theta_{13}$	$0.010 - 0.038$ $(0.013 - 0.040)$	

Table 1: The 3σ bounds on the parameters of the mass matrix $\mathcal{M}_\nu$, adopted from [3, 4, 18, 19]. Here $\Delta m_{ij}^2 = m_i^2 - m_j^2$. The boundaries for inverted hierarchy are the same as for the normal one, unless written explicitly. The range of $\sin^2 \theta_{13}$ is taken from the data of the Daya Bay experiment [18] (the values in parentheses – from RENO [19]).

3.2 Normal hierarchy

For normal hierarchy the explicit see-saw relation is

$$\text{diag}(0, \ m_2 e^{-2i\xi}, \ m_3)_{ij} = -\frac{\tilde{M}_{\text{D},i2}\tilde{M}_{\text{D},j3} + \tilde{M}_{\text{D},i3}\tilde{M}_{\text{D},j2}}{M_s} \ . \tag{8}$$

Diagonal components of this matrix equation give

$$\tilde{M}_{\text{D},12}\tilde{M}_{\text{D},13} = 0, \quad \tilde{M}_{\text{D},22}\tilde{M}_{\text{D},23} = \frac{1}{2}m_2 M_s e^{-2i\xi}, \quad \tilde{M}_{\text{D},32}\tilde{M}_{\text{D},33} = \frac{1}{2}m_3 M_s \ . \tag{9}$$

Using $m_2, m_3 \neq 0$ we find that $\tilde{M}_{\text{D},22}$, $\tilde{M}_{\text{D},23}$, $\tilde{M}_{\text{D},32}$, $\tilde{M}_{\text{D},33}$ are *all* non-zero. Analysis of non-diagonal terms reveals that *both* $\tilde{M}_{\text{D},12}$ and $\tilde{M}_{\text{D},13}$ are zero and there are two general solutions (c.f. [32]):

$$\tilde{M}_{\text{D},i2}^\pm = iz\sqrt{\frac{M_s}{2}}(0, \ \pm ie^{-i\xi}\sqrt{m_2}, \ \sqrt{m_3}), \quad \tilde{M}_{\text{D},i3}^\pm = iz^{-1}\sqrt{\frac{M_s}{2}}(0, \ \mp ie^{-i\xi}\sqrt{m_2}, \ \sqrt{m_3}) \ . \tag{10}$$

The solution $\tilde{M}_{\text{D}}^+$ with $\xi = \psi + \pi$ equals to $\tilde{M}_{\text{D}}^-$ with $\xi = \psi$. It allows us to consider only one solution $\tilde{M}_D^+$ on the interval $0 \leq \xi < 2\pi$. In what follows we therefore omit the superscript $+$.[4]

The mixing angles of the active-sterile neutrinos are defined as follows:

$$2\vartheta_\alpha^2 \equiv \sum_I |(M_{\text{D}}M_s^{-1})_{\alpha I}|^2 = \sum_I |(V^* \tilde{M}_{\text{D}}M_s^{-1})_{\alpha I}|^2 = \frac{1}{M_s^2}\sum_I |(V^* \tilde{M}_{\text{D}})_{\alpha I}|^2 \ . \tag{11}$$

Inserting the explicit solution (10) for $\tilde{M}_{\text{D}}$ results in

$$\vartheta_\alpha^2 = \frac{|z|^2}{4M_s}\left|\sqrt{m_3}V_{\alpha 3} - ie^{i\xi}\sqrt{m_2}V_{\alpha 2}\right|^2 + \frac{1}{4M_s|z|^2}\left|\sqrt{m_3}V_{\alpha 3} + ie^{i\xi}\sqrt{m_2}V_{\alpha 2}\right|^2 \ . \tag{12}$$

For $|z| \gg 1$ the contribution of $\tilde{M}_{\text{D},i3}$ is suppressed compared with that of $\tilde{M}_{\text{D},i2}$ and therefore we neglect the former (we will comment below on the case $|z| \gtrsim 1$).

---

[4]Unlike the parametrizations used e.g. in Ref. [17, 32, 33] this way of parametrizing the solution of the see-saw equations shows that there is only one branch of solutions, with all other related to it via redefinitions $N_2 \leftrightarrow N_3$ and shift of the Majorana phases. In particular in the parametrization we used it is much easier to analyze whether mixing angles become zero. The relation $|z| = \exp(\text{Im}\,\omega)$ holds, where the parameter ω was employed in [17].

As the value of the Majorana phase ξ is undetermined experimentally, the condition $\vartheta_\alpha = 0$ is satisfied iff $m_3|V_{\alpha 3}|^2 = m_2|V_{\alpha 2}|^2$ (we neglect second term on the r.h.s. of (12)). For the electron flavour ($\alpha = e$) it translates into

$$\sin^2\theta_{12}\frac{m_2}{m_3} = \tan^2\theta_{13}, \tag{13}$$

which, in principle, can be satisfied only for non-zero θ_{13}. This result has been already obtained in [17].

The bounds on the parameters of the mass matrix $\mathcal{M}_\nu$ at the 3σ level that we use are shown in Table 1. Note that in this paper we do not take into account statistical correlations between different oscillation parameters, allowing them to vary independently within their 3σ intervals. Consequently, we obtain the 3σ intervals for the combinations of parameters, entering Eq. (13)[5]:

$$\begin{aligned}
0.043 &< \sin^2\theta_{12}\tfrac{m_2}{m_3} < 0.070, \\
0.010(0.014) &< \tan^2\theta_{13} < 0.039(0.042),
\end{aligned} \tag{14}$$

They imply that the relation (13) *does not* hold exactly for the neutrino oscillation parameters, presented in Table 1. Therefore the mixing angle ϑ_e^2 cannot become zero, but has a non-trivial lower bound. To find the minimal value that it can reach, we consider the ratio of the angles $\vartheta_e^2/(\vartheta_e^2 + \vartheta_\mu^2 + \vartheta_\tau^2)$. Due to the unitarity of V, the denominator is

$$\sum_\alpha \vartheta_\alpha^2 \approx \frac{1}{2M_s^2}\sum_{\alpha,\beta,\gamma} V^*_{\alpha\beta}\tilde{M}_{\mathrm{D},\beta 2}V_{\alpha\gamma}\tilde{M}^*_{\mathrm{D},\gamma 2} = \frac{1}{2M_s^2}\sum_\beta \widetilde{|M_{\mathrm{D},\beta 2}|^2} = \frac{|z|^2}{4M_s}(m_2 + m_3). \tag{15}$$

Let us denote the ratio of the mixing of sterile neutrinos with one flavour to the sum of all mixings by T_α,

$$T_\alpha \equiv \frac{\vartheta_\alpha^2}{\sum\limits_\beta \vartheta_\beta^2}. \tag{16}$$

Then we get the following expression for T_e:

$$T_e = \frac{|ie^{i\xi}c_{13}s_{12}\sqrt{\frac{m_2}{m_3}} - s_{13}|^2}{1 + \frac{m_2}{m_3}}. \tag{17}$$

The minimum is achieved if we push θ_{12} and Δm_{21}^2 to their 3σ lower boundaries, θ_{13} and Δm_{31}^2 to their upper boundaries, and choose $\xi = -\pi/2$. The maximum is achieved when we set Δm_{31}^2 equal to its lower bound, θ_{13}, θ_{12} and Δm_{21}^2 to their upper bounds, and by choosing the Majorana phase $\alpha = \pi/2$. The bounds on T_e from Table 2 translate into the bound for the muon and tau flavours combined:

$$0.83 \leq T_\mu + T_\tau. \tag{18}$$

The minimum and maximum of different T_α are listed in the Table 2 and in Fig. 1.

This analysis was conducted in approximation of large $|z|$. See Appendix C for the account of finite-$|z|$ effects.

---

[5] Throughout this paper whenever two numbers are given instead of one, the first is based on the results of the Daya Bay experiment [18], and the second one (in parentheses) is obtained based on the result of application of the RENO bounds [19] (see Table 1).

Normal hierarchy	Inverted hierarchy	Normal hierarchy	Inverted hierarchy
$T_e \leq 0.15$	$0.02 \leq T_e \leq 0.98$	$T_e \leq 0.17$	$0.02 \leq T_e \leq 0.98$
$0.09 \leq T_\mu \leq 0.89$	$0 \leq T_\mu \leq 0.60$	$0.07 \leq T_\mu \leq 0.92$	$0 \leq T_\mu \leq 0.63$
$0.08 \leq T_\tau \leq 0.88$	$2 \times 10^{-4}\ (7 \times 10^{-5}) \leq T_\tau \leq 0.62$	$0.06 \leq T_\tau \leq 0.90$	$0 \leq T_\tau \leq 0.65$
The ranges are based on 2σ bounds		The ranges are based on 3σ bounds	

Table 2: The ratio of the sterile neutrino mixing with a given flavour α to the *sum* of the three mixings, T_α (defined by (16)). **Left** table shows the upper and lower values of T_α when parameters of neutrino oscillations are allowed to vary within their 2σ boundaries (taken from [3]). The **right** table shows the results when the parameters of active neutrino oscillations are varied within their 3σ limits (see Table 1). For the explanation of the numbers in parentheses, see Footnote 5.

3.3 Inverted hierarchy

Similarly to the previous case, for the inverted hierarchy we get a solution of the see-saw equations (7)

$$\tilde{M}_{\mathrm{D},i2} = iz\sqrt{\frac{M_s}{2}}(e^{-i\zeta}\sqrt{m_1},\ ie^{-i\xi}\sqrt{m_2},\ 0), \quad \tilde{M}_{\mathrm{D},i3} = iz^{-1}\sqrt{\frac{M_s}{2}}(e^{-i\zeta}\sqrt{m_1},\ -ie^{-i\xi}\sqrt{m_2},\ 0) \quad (19)$$

for $0 \leq \xi < 2\pi$. In this case ϑ_μ^2 or ϑ_τ^2 can become very suppressed, as we will show soon.

The mixing angles are

$$\vartheta_\alpha^2 = \frac{|z|^2}{4M_s}\left|\sqrt{m_1}V_{\alpha 1} - ie^{i(\xi-\zeta)}\sqrt{m_2}V_{\alpha 2}\right|^2 + \frac{1}{4M_s|z|^2}\left|\sqrt{m_1}V_{\alpha 1} + ie^{i(\xi-\zeta)}\sqrt{m_2}V_{\alpha 2}\right|^2. \quad (20)$$

For $|z| \gg 1$ they can become close to zero only if $\sqrt{m_1}|V_{\alpha 1}| = \sqrt{m_2}|V_{\alpha 2}|$. For $\alpha = \mu$ this condition translates into

$$|\tan\theta_{12} + \sin\theta_{13}\tan\theta_{23}e^{-i\phi}| = \sqrt{\frac{m_2}{m_1}}|1 - \sin\theta_{13}\tan\theta_{12}\tan\theta_{23}e^{-i\phi}|. \quad (21)$$

For the parameter set close to the best fit, left-hand side is *less* than the right-hand side, because then $\sin\theta_{13} \approx 0$, while $\tan\theta_{12} < 1$ and $m_1 \approx m_2$. To attain the equality one has to push left-hand side up and the right-hand side down. $\phi = 0$ makes phases of both complex terms inside $|...|$ on the left-hand side equal, thereby the absolute value of their sum becomes maximal. Simultaneously the right-hand side becomes minimal. For this specific choice of the Dirac angle the equality (21) turns into

$$\frac{\sqrt{\frac{m_2}{m_1}} - \tan\theta_{12}}{\sqrt{\frac{m_2}{m_1}}\tan\theta_{12} + 1} = \sin\theta_{13}\tan\theta_{23}. \quad (22)$$

The 3σ bounds for inverted hierarchy in general are the same as for the normal one (see Table 1) with the exception of the "atmospheric" mass difference, that slightly differs. Using these values we find

$$0.14 < \frac{\sqrt{\frac{m_2}{m_1}} - \tan\theta_{12}}{\sqrt{\frac{m_2}{m_1}}\tan\theta_{12} + 1} < 0.24, \quad 0.08\ (0.09) < \sin\theta_{13}\tan\theta_{23} < 0.26. \quad (23)$$

We see that two regions overlap, therefore the relation (21) can be satisfied and ϑ_μ^2 can be zero in a wide region of values of the parameters of the neutrino oscillation matrix. See, however, Sec. 3.4 below.

Similarly, the condition $\vartheta_\tau = 0$ (for $\phi = \pi$) translates into

$$\frac{\sqrt{\frac{m_2}{m_1}} - \tan\theta_{12}}{\sqrt{\frac{m_2}{m_1}}\tan\theta_{12} + 1} = \sin\theta_{13}\cot\theta_{23}, \tag{24}$$

and can be satisfied, because the quantity on the right hand side varies from 0.07 (0.09) to 0.24 (0.25), well within the range of (23).[6]

On the other hand, ϑ_e can be zero only if

$$\cot\theta_{12} = \sqrt{\frac{m_2}{m_1}} \tag{25}$$

can be realized. The left hand side is always larger than the right hand side (within the 3σ region), therefore no ϑ_e suppression can occur. However it is important to know what minimal value this mixing angle can reach. According to Eq.(20) electron mixing angle is given by

$$\vartheta_e^2 = \frac{|z|^2}{4M_s}\cos^2\theta_{13}\left(m_1\cos^2\theta_{12} + m_2\sin^2\theta_{12} + \sin(\xi - \zeta)\sin 2\theta_{12}\sqrt{m_1 m_2}\right). \tag{26}$$

For $\xi - \zeta = -\pi/2$ this quantity is minimal

$$\vartheta_{e,min}^2 = \frac{|z|^2}{4M_s^2}\cos^2\theta_{13}\left(\sqrt{m_1}\cos\theta_{12} - \sqrt{m_2}\sin\theta_{12}\right)^2. \tag{27}$$

To compare it with the other mixing angles, we note that the relation

$$\sum_\alpha \vartheta_\alpha^2 \approx \frac{|z|^2}{4M_s}(m_1 + m_2) \tag{28}$$

holds (similar to Eq.(15) in the case of normal hierarchy). Therefore

$$\frac{\vartheta_{e,min}^2}{\sum_\alpha \vartheta_\alpha^2} = \frac{\cos^2\theta_{13}}{1 + \frac{m_2}{m_1}}\left(\cos\theta_{12} - \sqrt{\frac{m_2}{m_1}}\sin\theta_{12}\right)^2. \tag{29}$$

The results of the analysis are listed in Table 2 and Fig. 1. From the upper bound on T_α we derive the bound

$$T_\mu + T_\tau \geq 0.02 . \tag{30}$$

We see that in this mass hierarchy it is possible for the overall coupling of the sterile neutrino to both μ and τ flavours to become tiny compared to the electron flavour coupling.

---

[6]It was pointed out in [17] that both ϑ_μ and ϑ_τ can be suppress in inverted hierarchy, for $\theta_{13} = 0$. For this to happen the relation $\sqrt{\frac{m_2}{m_1}} = \tan\theta_{12}$ should hold, as one can also see from Eqs. (22) and (24). The corresponding value of θ_{12} is however well outside the 3σ interval. The general case $\theta_{13} \neq 0$ has not been analyzed in [17].
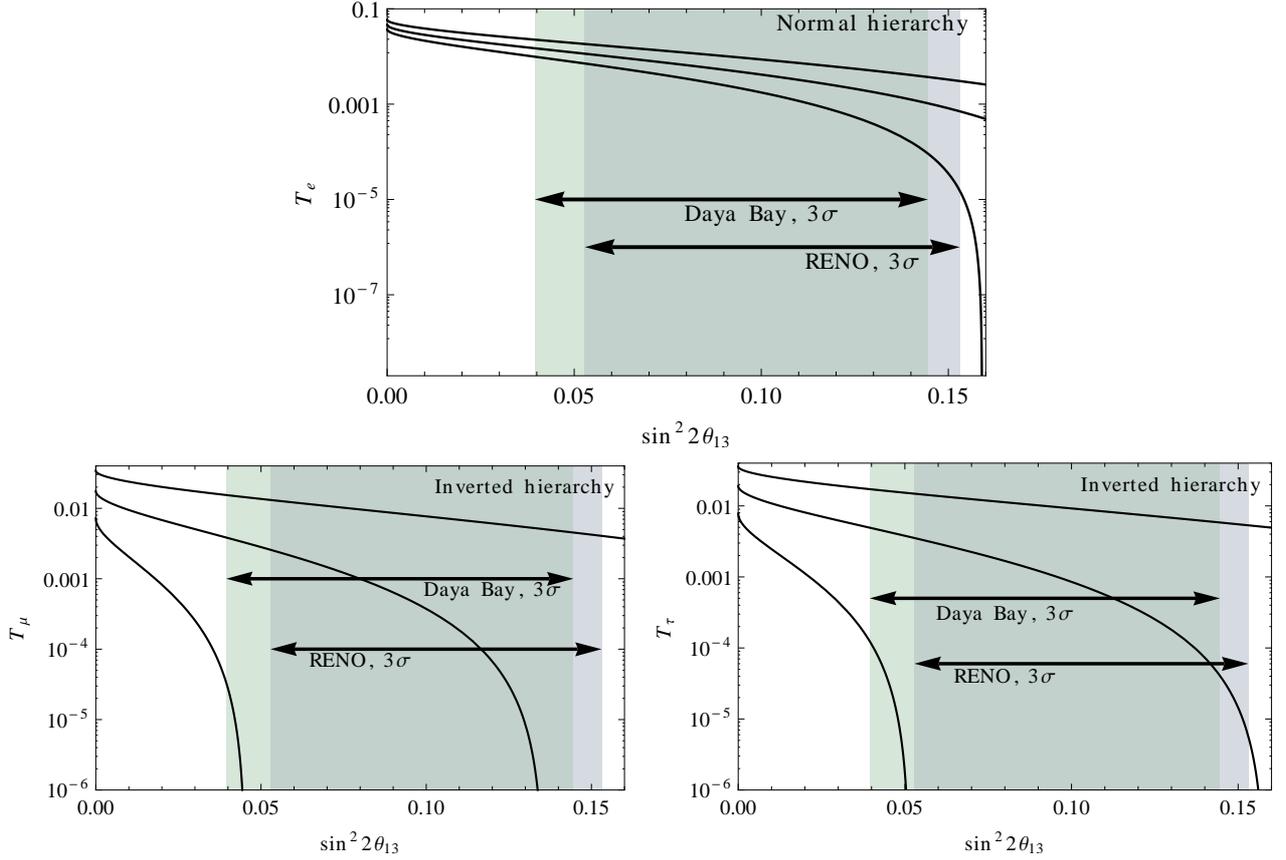
Figure 1: The minimal ratios of mixing angles $T_\alpha = \vartheta_\alpha^2 / \sum \vartheta_\beta^2$. **The upper** figure depicts normal hierarchy, **two lower** ones – IH. In all figures, the lower curve corresponds to the choice of the mixing angles and mass splittings that minimizes the ratio within the 3σ range, upper – that maximizes it, middle employs the best-fit parameters (for details of the choices, see Secs. 3.2, 3.3). CP-phases are $\xi = -\pi/2$ for the T_e-plot, $\phi = 0$, $\xi - \zeta = \pi/2$ for T_μ, and $\phi = \pi$, $\xi - \zeta = -\pi/2$ for T_τ. The bands *Daya Bay* and *RENO* correspond to the 3σ ranges of θ_{13}, indicated by the corresponding experiments [18, 19].

Flavour α	$(\vartheta_\alpha^2)_{\min}$ @ 1 MeV	$|z|$
e	7×10^{-10}	2.2 (2.4)
μ, τ	10^{-8}	1.5

(a) NH, best-fit

Flavour α	$(\vartheta_\alpha^2)_{\min}$ @ 1 MeV	$|z|$
e	10^{-10} (4×10^{-11})	6.2 (9.8)
μ	8×10^{-10} (6×10^{-10})	5.4 (6.3)
τ	1.2×10^{-9} (1.0×10^{-10})	4.6 (5.1)

(b) NH, 3σ

Flavour α	$(\vartheta_\alpha^2)_{\min}$ @ 1 MeV	$|z|$
e	10^{-8}	2.3
μ, τ	2×10^{-9}	3.5

(c) IH, best-fit

Flavour α	$(\vartheta_\alpha^2)_{\min}$ @ 1 MeV	$|z|$
e	6×10^{-9}	2.7
μ, τ	see text	

(d) IH, 3σ

Table 3: Minimal values of the active-sterile mixing angles ϑ_α^2, obtained using the best-fit values of neutrino oscillation parameters or by varying the neutrino oscillation data within their 3σ intervals, listed in Table 1. The values for $(\vartheta_\alpha^2)_{\min}$ are provided for sterile neutrinos with the mass $M_s = 1$ MeV. For other masses one should multiply them by (MeV$/M_s$). Columns "$|z|$" show the values of $|z|$ for which the minimum in (31) is reached. For the explanation of numbers in brackets, see Footnote 5.

3.4 Minimal mixing angles in the νMSM

Finally, we find the *minimal* values of the sterile neutrino mixing angles in the νMSM, compatible with the neutrino oscillation data. These angles will turn out to be much smaller than the experimental upper bounds in all regions of masses, probed by the experiments. A general solution of the see-saw equations (12), (20) gives ϑ as a function of $|z|$:

$$\vartheta_\alpha^2 = A_\alpha |z|^2 + \frac{B_\alpha}{|z|^2} \tag{31}$$

with coefficients A_α and B_α independent of $|z|$. The minimum of this expression is reached for $|z|_\alpha^2 = \sqrt{B_\alpha/A_\alpha} \geq 1$ and is given by

$$(\vartheta_\alpha^2)_{\min} = 2\sqrt{A_\alpha B_\alpha}. \tag{32}$$

To find an *absolute* lower bound on the mixing angle for a given sterile neutrino mass, we vary this expression over the parameters of neutrino oscillations. The resulting mixing angles and the corresponding values of $|z|$ are listed in Table 3.[7] One can see that the values presented therein do not depend significantly on the 3σ upper bound on θ_{13} that we choose. The only exception is the minimum of the ϑ_e angle. In this case the exact value of the upper bound on θ_{13} defines how close A_α, and hence $(\vartheta_\alpha^2)_{\min}$, can come to zero.

For the mixing angles $\vartheta_{\mu,\tau}^2$ in the case of inverted hierarchy $A_\alpha = 0, B_\alpha \neq 0$ and formally for infinitely large $|z|$ they would become zero. The value of $|z|$, however, is bounded from above,

---

[7]Notice, that the ratio of the mixing angles $\vartheta_\alpha^2/\vartheta_\beta^2$ does not reach its minimum when (32) is satisfied. The values of $|z|$ for which the bounds on the lifetime are relaxed the most are those when some of the mixing angles reach their upper experimentally allowed value.

$|z| < z_{\max}$, by the requirement that *none of three* mixing angles exceeds its upper bound (for quantitative estimates of $z_{\max}$, look at Fig. 9). Therefore the couplings to μ and τ neutrinos remain *finite*. Estimates of mixing angles can be provided for B_α given by L_α^{IH} (46,47), along with $A_{\mu,\tau} = 0$, $z = z_{\max}$

$$\vartheta_{\mu,\tau}^2 \gtrsim 2 \times 10^{-8} \frac{\text{MeV}}{M_s z_{\max}^2}, \qquad \text{(IH)} \tag{33}$$

4 Experimental bounds on sterile neutrino mixings

The direct experimental searches for neutral leptons had been performed by a number of collaborations [34–46] (see e.g. [11, 12] for review of various constraints). The negative results of the searches are converted into the *upper* bound on $\vartheta_\alpha \vartheta_\beta$ for different flavours. If neutrino oscillations are mediated by these sterile neutrinos, these bounds can be translated into the *upper* bounds on parameter $|z|$ and *lower* bounds on sterile neutrino lifetime.

Below, we take a closer look at two main types of experiments ("peak searches" and "fixed target experiments")[8] and describe *reinterpretation of these bounds* in the case, when sterile neutrinos with MeV–GeV masses are also responsible for neutrino oscillations.

4.1 Peak searches

In "*peak search*" experiments [49–52], one considers the two-body decay of charged π or K mesons to charged lepton ($e^\pm$ or $\mu^\pm$) and neutrino (see e.g. [11] for discussion). In case of the pion decay the limit on ϑ_e^2 for masses in the range $60\,\text{MeV} \le M_s \le 130\,\text{MeV}$ is provided by the searches for the secondary positron peak in the decay $\pi^+ \to e^+ N$ to the massive sterile neutrino N as compared to the primary peak coming from the $\pi^+ \to e^+ \nu_e$ decay. Recent analysis of [45] puts this limit at $\vartheta_e^2 < 10^{-8}$ in the mass range $60 - 129\,\text{MeV}$, for earlier results see [36, 37]. In the smaller mass region ($4\,\text{MeV} \lesssim M_s \lesssim 60\,\text{MeV}$) Refs. [36, 37] provided the bound based on the change of the number of events in the primary positron peak located at energies $M_\pi/2$. Similar bounds were obtained for the same mixing angle in studies of *kaon* decays [40] and for the ϑ_μ^2 in the decays of both pions [42–44] and kaons [40, 41].

The *lower* bound on the sterile neutrino lifetime τ_s in the model (4), based on the peak search data and neutrino oscillations is shown in Fig. 2 by dot-dashed green lines. The parameters of neutrino mixing matrix are allowed to vary within their 3σ limits (to minimize τ_s, while still keeping the values of all mixing angles compatible with the bounds from direct experimental searches).

4.2 Fixed target experiments and neutral currents contribution

The second kind of experiments ("*fixed target experiments*") [35, 38, 39] aims to create sterile neutrinos in decays of mesons and then searches for their decays into pairs of charged particles. Notice, that the expected signal in this second case is proportional to ϑ_α^4 or $\vartheta_\alpha^2 \vartheta_\beta^2$ (and not to ϑ_α^2 as in the case of peak searches, discussed in the Section 4.1). We will demonstrate below that in the models like (4) (and in particular in the νMSM) the results of some fixed

---

[8]The neutrinoless double-beta decay ($0\nu\beta\beta$) does not provide significant restrictions on the parameters of the sterile neutrinos in the type-I see-saw models (contrary to the case discussed in e.g. [11]), see discussion in [17, 47]. In particular, this is the case in the νMSM [48].
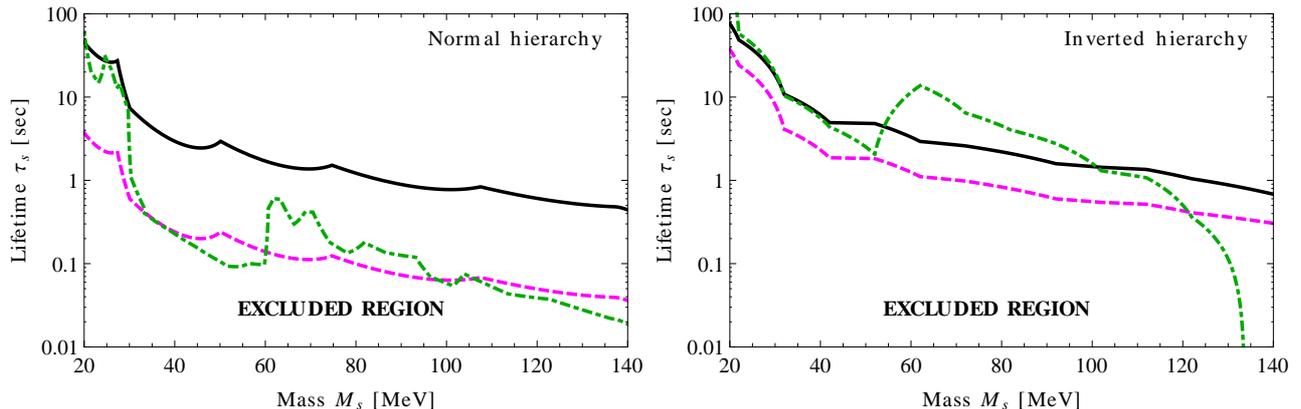
Figure 2: The lower bounds on the lifetime of sterile neutrinos, responsible for the mixings between active neutrinos of different flavours in the see-saw models (4). The bounds are based on the combination of negative results of direct experimental searches [34, 35, 37, 40–45] with the neutrino oscillation data [3]. The neutrino oscillation parameters are allowed to vary within their 3σ confidence intervals to minimize the lifetime. The solid black curve is based on our reinterpretation of PS191 data *only*, that takes into account charged and neutral current contributions (see Sec. 4.3). The interpretation of the PS191 experiment, taking into account only CC interactions (used e.g. in the previous works [12, 17]) is shown in magenta dashed line. The bound from peak searches experiments *only* [37, 40–45] is plotted in green dot-dashed line.

target experiments should be reinterpreted and will provide stronger bounds than discussed in previous works [11, 12, 17] (see also [53]).

4.3 Reinterpretation of the PS191 and CHARM experiments

The experiment **PS191** at CERN was a "fixed target" type of experiment described above [34, 35]. In searches for sterile neutrinos lighter than the pion $M_s < M_\pi$, the pair of charged particles that were searched for in the neutrino decay comprised mostly of electron and positron:

$$
\begin{aligned}
\pi^+/K^+ \to e^+ + \ &N \\
&\hookrightarrow e^+ e^- \nu_\alpha \,,
\end{aligned}
\tag{34}
$$

where N is a sterile neutrino with the mass M_s. The first reaction in the chain is solely due to the *charged-current* (CC) interaction, and its rate is proportional to the ϑ_e^2.

If sterile neutrinos interact through both *charged and neutral currents* (CC+NC) as it is the case in the models with the see-saw Lagrangian (4), any of three active-neutrino flavours may appear in the decay of N in (34). The decay widths are [49]:

$$
\Gamma(N \to e^+ e^- \nu_\alpha) = c_\alpha \vartheta_\alpha^2 \frac{G_F^2 M_s^5}{96\pi^3},
\tag{35}
$$

with the following definition[9]

$$
c_e = \frac{1 + 4\sin^2\theta_W + 8\sin^4\theta_W}{4}, \quad c_\mu = c_\tau = \frac{1 - 4\sin^2\theta_W + 8\sin^4\theta_W}{4},
\tag{36}
$$

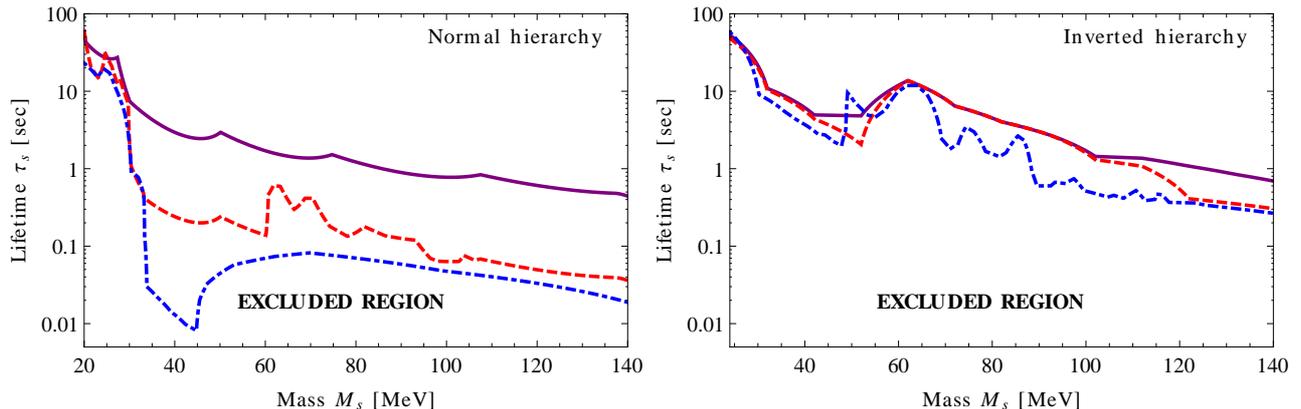[9]Note that in the Ref. [54] there is a typo in the expression for c_τ (Eq. (2)).

Figure 3: Comparison with the previous bounds on sterile neutrino lifetime in the νMSM [17]. The solid purple curves represent the results of the present work, obtained by the combination of peak searches experiments [37, 40–45] together with the reanalysis of PS191, that takes into account neutral currents (a union of black and green bounds from Fig. 2). The red dashed curve is based on the combination of the same peak searches with the *original* interpretation of PS191 (i.e., with charged current interactions only). The blue dot-dashed line is taken from [17]. *Notice*, that the results of [17] were multiplied by a factor 2 to account for the Majorana nature of the particles (see discussion in Sec. 4.4), that was missing therein. The difference between the red and blue lines in the case of normal hierarchy is explained by wider 3σ intervals for neutrino oscillation data, used in [17], compared to our work.

and θ_W is the Weinberg's angle so that $\sin^2\theta_W \approx 0.231$ and $c_e \approx 0.59$, $c_{\mu(\tau)} \approx 0.13$. Therefore, the total number of events inside the detector that registers electron-positron pairs would be proportional to the combination of mixing angles $\vartheta_e^2 \times (\sum c_\alpha \vartheta_\alpha^2)$.

However, the model employed in the interpretation of the PS191 experiment [34, 35] was different, as has already been pointed in [53]. In the original analysis it was assumed that sterile neutrino interacts *only via charged currents*, but not through neutral currents. In our language it means that $c_e = 1, c_{\mu(\tau)} = 0$ was used instead of the values (36)[10]. As was noticed above, the probability of meson decay into sterile neutrino does not alter if we exclude the neutral-current interaction, and therefore the total number of events with the electron-positron pair would be proportional to $\vartheta_e^2 \times \vartheta_e^2$.

Therefore if we denote the bounds listed in [34, 35] as $\vartheta_e^4 \leq \vartheta_{e(exp)}^4$, then the bound for the νMSM takes form

$$\vartheta_e^2 \left(\sum_{\alpha=\{e,\mu,\tau\}} c_\alpha \vartheta_\alpha^2 \right) \leq \vartheta_{e(exp)}^4 . \tag{37}$$

Similar bounds can be extracted from the reanalysis of meson decays into *muon* and sterile neutrino, that leads to replacement $e \to \mu$ in (37). As a result, the reinterpretation of the results of the PS191 experiment in combination with neutrino oscillation data produces up to an order of magnitude *stronger* bounds on lifetime than in the previous works (see Figs. 2 and 3).

Similarly, the CHARM experiment [39] provided bounds on the mixing angles of sterile

---

[10]Model described in [34, 35] contains only one Dirac neutrino, while in the νMSM we have two Majorana fermions. Therefore actually $c_e = 1/2$ in the original model. For details see Sec. 4.4
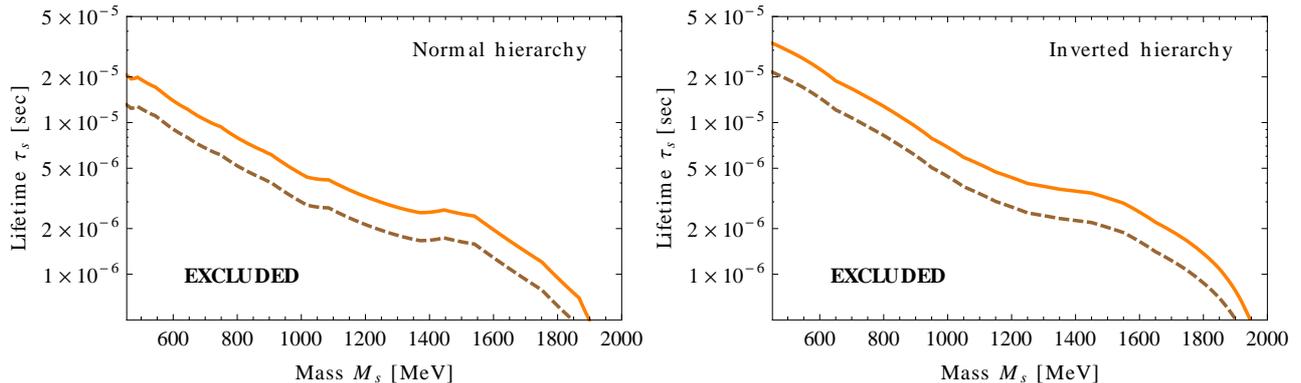
Figure 4: Comparison of the bounds on sterile neutrino lifetime (in the model (4)) based on the results of the CHARM experiments [39] *solely* (combined with the neutrino oscillation data). The orange (upper) curves correspond to the model with charged and neutral current interactions of sterile neutrinos, the brown (lower) – to the model with charged current interactions only. For details, see Sec. 4.3.

neutrinos in the mass range $0.5\,\text{GeV} \lesssim M_s \lesssim 2\,\text{GeV}$. In the original analysis NC contributions *were neglected*. Therefore, to apply the results of this experiment to the case of the νMSM, we reanalyzed the data as described above. In Fig. 4 we compare lifetime bounds coming from the CHARM experiment solely for CC and CC+NC interactions of sterile neutrinos. The difference in this case is about a factor of 2.[11]

4.4 A note on Majorana vs Dirac neutrinos

For completeness we briefly discuss the difference in interpreting experimental results for *Majorana vs. Dirac sterile neutrinos*. Similar discussion can be found e.g. in [12]. When interpreting the experimental results one should take into account that in present work we consider *two Majorana sterile neutrinos*, while the experimental papers often phrase their bounds in terms of the mixing with a single *Dirac* neutrino, that we will denote U_α^2. In the νMSM twice more sterile neutrinos are produced per single reaction (because there are two sterile species – N_2 and N_3), and, owing to their Majorana nature, each sterile neutrino decays twice faster (additional charge-conjugated decay modes are present). Notice, that the mass splitting between between two sterile states N_2, N_3 is small $|M_2 - M_3| \ll \frac{1}{2}(M_2 + M_3) = M_s$ and once born, the states oscillate fast into each other. Averaging over many oscillations can be accounted for by an extra factor $\frac{1}{2}$ in the number of N_2 and N_3 species. Therefore, for fixed target experiments one gets the same number of the detector events involving one Dirac sterile neutrino as one gets in the νMSM if $(\vartheta_{\alpha 2}^2 + \vartheta_{\alpha 3}^2)^2 = U_\alpha^4$. That is, one should identify $2\vartheta_\alpha^2$ with the measured U_α^2 (recall (11) that $\vartheta_\alpha^2 = \frac{1}{2}(\vartheta_{\alpha 2}^2 + \vartheta_{\alpha 3}^2)$). In the case of peak searches, the bound U_α^2 should be interpreted in the νMSM as $\vartheta_{\alpha,2}^2 + \vartheta_{\alpha,3}^2 \le U_\alpha^2$, as production of *any* state

---

[11]In the case of the PS191 experiment, when using CC only for masses below the mass of pion suppression of the ϑ_e^2 mixing angle due to neutrino oscillations meant that instead of ϑ_e^2 bounds the lifetime is defined by the (much weaker) ϑ_μ^2 bounds. That led to the significant relaxation of the lower bound on the lifetime. If NC were taken into account, this was not possible anymore and therefore the lower bound on sterile neutrino lifetime became stronger by as much as the order on magnitude (black vs. magenta curve on the left panel in Fig. 2. In case of the CHARM experiment, both ϑ_e^2 and ϑ_μ^2 are strongly constrained and switching from one constraint to another makes (numerically) much smaller difference.

(a) Bound on the combination $\vartheta_e\sqrt{\sum c_\alpha \vartheta_\alpha^2}$ (b) Bound on the combination $\vartheta_\mu\sqrt{\sum c_\alpha \vartheta_\alpha^2}$
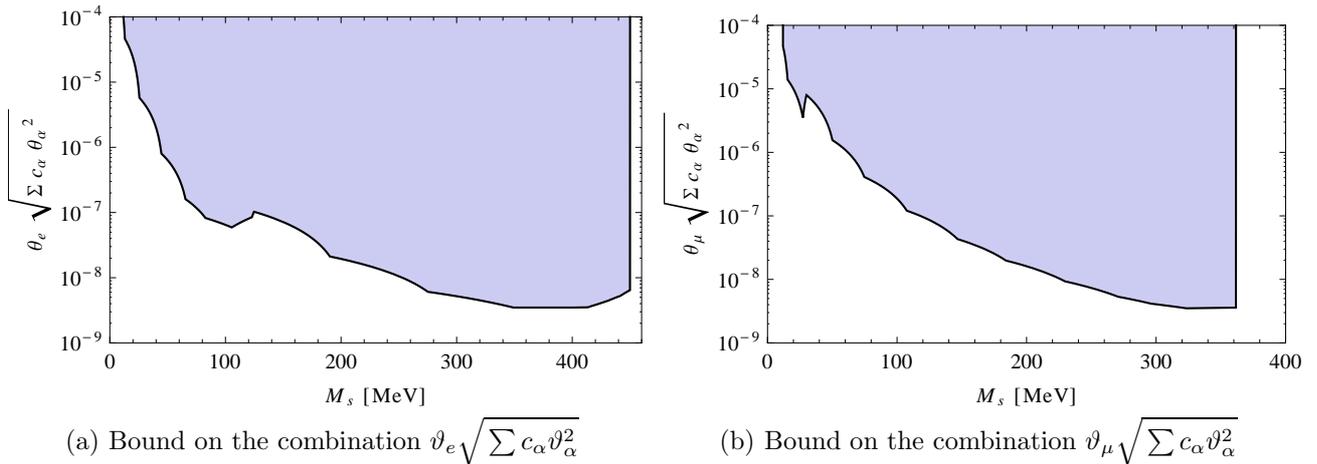
Figure 5: Direct accelerator bounds on the combination of active-sterile neutrino mixing angles, resulting from the reanalysis of the PS191 experiment [34, 35], taking into account decays of sterile neutrino through both charged and neutral currents and their Majorana nature. The shaded region is excluded. The case, analyzed in the original works [34, 35] (decay of sterile neutrino through the charged current only) corresponds to the choice $c_e = 1$, $c_\mu = c_\tau = 0$, for details, see Sec. 4.3. We plot the bounds for *two Majorana* neutrinos (as in Fig. 6) while in the original works [34, 35] a single Dirac neutrino was analyzed.

N_2 or N_3 contributes to the number of events in the secondary peak, i.e. again $2\vartheta_\alpha^2$ should be identified with U_α^2. Notice, that this factor 2 is missing in [17].

5 Results

In this Section we summarize our results: the upper bound on the (combination of) mixing angles of sterile and active neutrinos in the see-saw models (2) in the range 10 MeV – 2 GeV and the lower bound on sterile neutrino lifetime, obtained in combination of these bounds with constraints, coming from neutrino oscillation data.

5.1 Bounds on the mixing angles of sterile neutrinos

For the models (4) (two Majorana sterile neutrinos, interacting through both charged and neutral interactions), the compilation of constraints on various combinations of active-sterile mixing angles $(\vartheta_e^2,\ \vartheta_\mu^2,\ \vartheta_e\sqrt{\sum c_\alpha\vartheta_\alpha^2},\ \vartheta_\mu\sqrt{\sum c_\alpha\vartheta_\alpha^2})$ that we used in this work are plotted in Figs. 5 and 6.[12]

5.2 The lower bound on the lifetime of sterile neutrinos

The result of the Sections 3.2–3.3, combined with these experimental bounds can be translated into the *lower* limits on the lifetime of sterile neutrinos. These results are presented in Figs. 7 on page 17. Additionally, we plot the lifetime bounds for the best-fit values of the PMNS parameters yet with $\theta_{13} = 0$ (as used e.g. in [12, 31]). For normal hierarchy we see that

---

[12]Notice that in the published results of the PS191 experiment [35] bounds are given up to $M_s = 400$ MeV. We extend these bounds up to 450 MeV, using the PhD Thesis of J.-M. Levy [55].
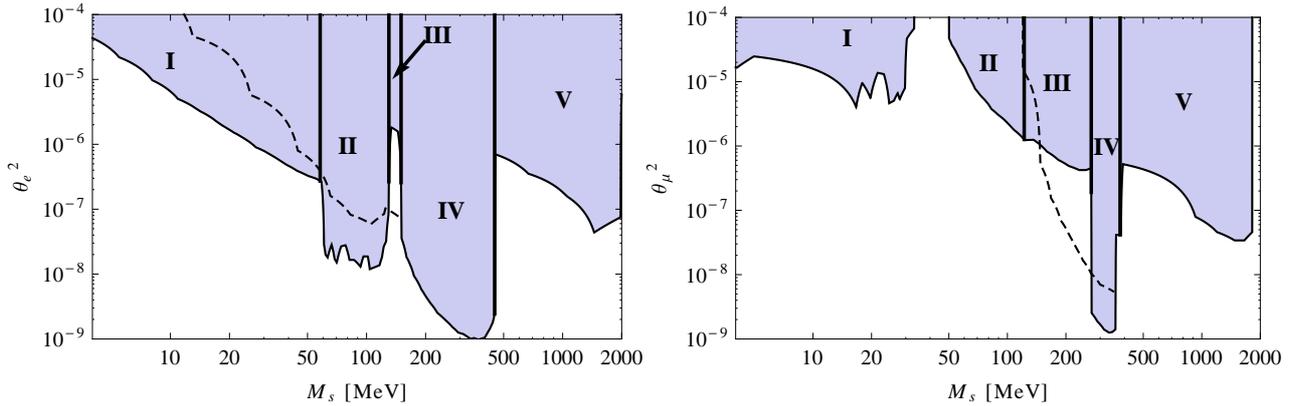
Figure 6: Direct accelerator bounds on the mixing angles. **Left panel:** ϑ_e^2 bounds, taken from [37] (region I), [45] (region II), [40] (region III), [35, 55] (region IV) and [39] (region V). **Right panel:** ϑ_μ^2 bounds, taken from [42–44] (region I), [40](region II), [41] (region III), [35](region IV) and [38] (region V). The shaded regions are ruled out by the experimental findings. Dashed curves indicate mixing angle bounds given by original interpretation of PS191 experiment, but we *do not* use them to derive our final results, as explained in Sec. 4.3. The bounds are shown for the Majorana neutrino and are therefore two times *stronger* (see Section 4.4), while in the original works [34, 35] a single Dirac neutrino has been considered.

our bounds with $\theta_{13} \neq 0$ are relaxed by as much as the order of magnitude at some masses, compared to $\theta_{13} = 0$ case. The difference for IH is not so pronounced. *Notice*, that the bounds of [12, 17, 31] were different from what we show as dashed line in Fig. 7 because of ignoring the neutral current contributions to the results of PS191 experiment (for details see discussion in Section 4 and Figs. 2, 3).

6 Discussion

In this work we have investigated experimental restrictions on the parameters of the see-saw Lagrangian in the case when two sterile neutrinos with the masses between ~ 10 MeV and 2 GeV are responsible for neutrino oscillations. Combined with the results of the direct experimental searches, the neutrino oscillation data provide stringent lower bounds on their lifetime, τ_s and allows to determine both *maximum* and *minimum* values of the mixing angles ϑ_α^2.

We have reinterpreted the results of the PS191 experiment [34, 35], following [53], by taking into account not only charged, but also neutral-current interactions (as both of these are present in the Type I see-saw Lagrangian). Our results demonstrated that below the mass of the pion the fixed target experiments (ϑ^4 experiments) provide *stronger* restrictions than the peak search experiments (ϑ^2 experiments) in case of *normal hierarchy*. In *inverted hierarchy* the reanalysis of the PS191 experiment turns out to be very important as well. In the original analysis of the CHARM experiment [38] neutral-current contributions were neglected as well and we have reinterpreted these results in a similar way to PS191. The final results are presented in Figs. 7.
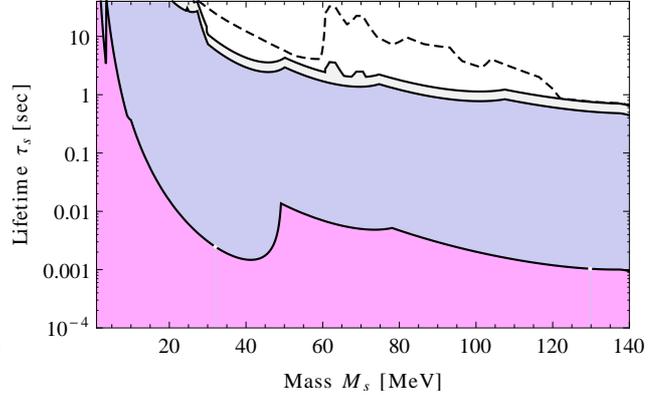
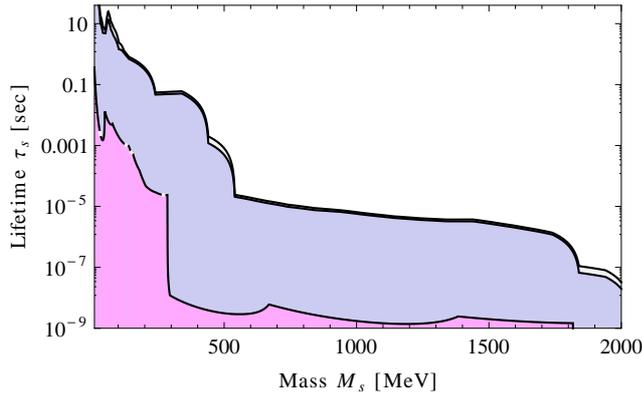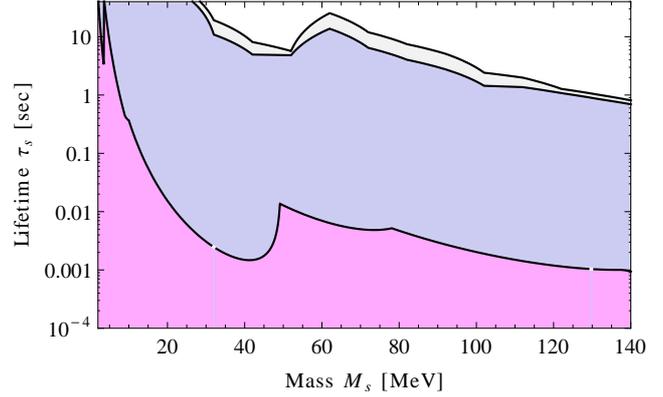Future experiments (for example, NA62 in CERN [13], LBNE experiment in FNAL[14] or

---

[13]http://na62.web.cern.ch/NA62
[14]http://lbne.fnal.gov
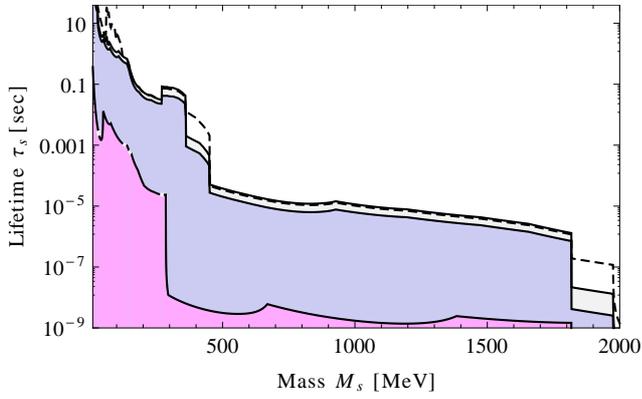
(a) Normal hierarchy, mass range $10\,\mathrm{MeV} - 2\,\mathrm{GeV}$

(b) Normal hierarchy, zoom at the mass range $10\,\mathrm{MeV} - 140\,\mathrm{MeV}$

(c) Inverted hierarchy, mass range $10\,\mathrm{MeV} - 2\,\mathrm{GeV}$

(d) Inverted hierarchy, zoom at the mass range $10\,\mathrm{MeV} - 140\,\mathrm{MeV}$

Figure 7: The resulting lower bounds on sterile neutrino lifetime τ_s as a function of their mass, obtained by requiring that two Majorana sterile neutrinos are responsible for neutrino oscillations and their parameters do not contradict the negative results of direct experimental searches. In all figures the upper curve comes from using of the best fit neutrino oscillation parameters, the middle one – from their variation within the 3σ limits, and the lower one does not take into account neutrino oscillation data and puts all three mixing angles equal to their direct experimental bounds. The dashed line for NH corresponds to the best-fit values of PMNS parameters with $\theta_{13} = 0$ and shows how much the bounds on the lifetime relax for non-zero value of θ_{13} (see text, Section 5 for discussion).

17

upgraded LHCb experiment) have a great potential of discovering light neutral leptons of the νMSM or significantly improving the bounds on their parameters (see discussion in [56] and [57]). Due to the strong suppression of the mixing angles ϑ_e^2 in the case of NH and ϑ_μ^2 in the case of IH, the peak searches in the kaon decays (such as e.g. [58]) may miss the sterile neutrino (cf. [17]).[15]

Finally, sterile neutrinos with the masses in MeV–GeV region and small mixing angles can play significant role in the early Universe (for a review see [16]). Due to their small mixing angles, the lifetime of sterile neutrinos can be long enough for them to be present in primordial plasma at $\sim$ MeV temperatures, affecting the Big Bang nucleosynthesis (BBN) (for more details and references, see [14, 15, 22]). Comparison of the 3σ lower bounds from the direct searches with the 3σ *upper* bounds from BBN on the lifetime of sterile neutrinos (based on [22]) is presented in Fig. 8. There are no allowed values of sterile neutrinos lifetimes for $10\,\mathrm{MeV} \lesssim M_s < 140\,\mathrm{MeV}$ for both types of hierarchies (i.e. the upper bound is *smaller* than the lower bound, see the purple double-shaded region in Fig. 8). This conclusion is based on the weakest BBN bound, based on the primordial Helium-4 abundance as determined from CMB observations [6, 61], which presently has large error bars. The astrophysical measurements (e.g. [62, 63]) provide a much tighter bounds on the Helium-4 abundances, further lowering the upper bound from BBN by as much as the order of magnitude (see [22] for discussion). It should be stressed that adopting the BBN bounds from the previous works [14, 15] would lead to essentially the same conclusion.

Our conclusion differs from that of [17], where it was argued that in the case of normal hierarchy there is an open region of parameter space compatible with both direct experimental searches and BBN bounds of [15]. This difference comes mainly from the reanalysis of the data of PS191 experiment that was carried out in the present paper (as illustrated in Fig. 3).

For heavier sterile neutrinos, no reliable computations of the sterile-neutrino impact on BBN were made up to the present time, and the rough estimate $\tau_s \lesssim 0.1\,\mathrm{sec}$ is usually used instead (for more details, see [15]). This latter bound gives no substantial restriction on such heavy sterile neutrinos, since from Fig. 7 it can be inferred that the horizontal line $\tau_s = 0.1\,\mathrm{sec}$ is generally *higher* than the bounds depicted there.

Apart from their influence on BBN, the decays of sterile neutrinos may produce additional entropy and energy of plasma [22, 64]. Their out-of-equilibrium behaviour may lead as well to the successful baryogenesis scenario [29, 31, 65]; the generation of large lepton asymmetry at temperatures below the sphaleron freeze-out [13]. In Fig. 9 we superimpose the bounds on $|z|$, coming from the direct experimental searches on the region of parameters $(|z|,\,M_s)$ in which the successful baryogenesis is possible (the region inside the black contours marked "BAU" based on the Ref. [31]). Additionally, the lepton asymmetry may be generated at $T \lesssim$ few GeV [13] and can affect production of dark matter sterile neutrinos [66, 67]. Sterile neutrinos with the mass of about 200 MeV and mixing angles $\sim 10^{-7} - 10^{-8}$ can affect the physics of supernova explosions [68]. Finally, our constraints may affect the low-reheating temperature cosmological scenario (see e.g. [69, 70]).

---

[15]GeV-scale sterile neutrinos in the models with extended Higgs sector [59] can be searched at the LHC [60].
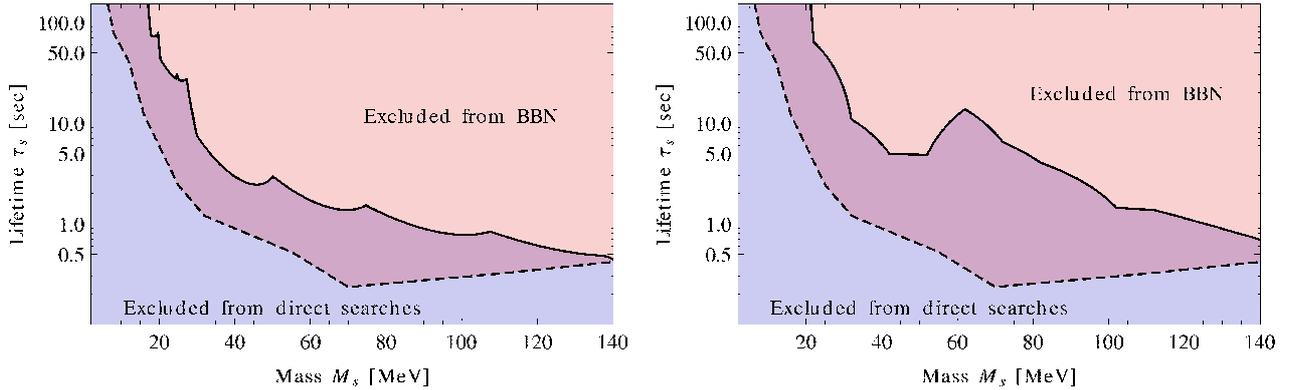
Figure 8: Experimental *lower* bounds on the lifetime of sterile neutrinos (solid line), combined with the *upper* bounds coming from the BBN (dashed line) [22]. **Left panel:** normal hierarchy, **right panel:** inverted hierarchy. Shown are 3σ lower bounds from the Fig. 7 and the weakest bound from primordial nucleosynthesis (based on the CMB measurements of primordial Helium abundance, yielding $Y_p = 0.445$ at the 3σ level [6, 61], see text for details).

References

[1] A. Strumia and F. Vissani, *Neutrino masses and mixings and.*, `hep-ph/0606054`.

[2] T. Schwetz, M. Tortola and J. W. F. Valle, *Three-flavour neutrino oscillation update*, *New J. Phys.* **10** (2008) 113011 [`0808.2016`].

[3] T. Schwetz, M. Tortola and J. Valle, *Where we are on θ_{13}: addendum to 'Global neutrino data and recent reactor fluxes: status of three-flavour oscillation parameters'*, *New J.Phys.* **13** (2011) 109401 [`1108.1376`].

[4] G. L. Fogli, E. Lisi, A. Marrone, A. Palazzo and A. M. Rotunno, *Evidence of theta(13)¿0 from global neutrino data analysis*, *Phys.Rev.* **D84** (2011) 053007 [`1106.6028`].

[5] **Particle Data Group** Collaboration, K. Nakamura *et. al.*, *Review of particle physics*, *J.Phys.G* **G37** (2010) 075021.

[6] E. Komatsu, K. M. Smith, J. Dunkley, C. L. Bennett, B. Gold, G. Hinshaw, N. Jarosik, D. Larson, M. R. Nolta, L. Page, D. N. Spergel, M. Halpern, R. S. Hill, A. Kogut, M. Limon, S. S. Meyer, N. Odegard, G. S. Tucker, J. L. Weiland, E. Wollack and E. L. Wright, *Seven-year Wilkinson Microwave Anisotropy Probe (WMAP) Observations: Cosmological Interpretation*, ApJS **192** (Feb., 2011) 18–+ [`1001.4538`].
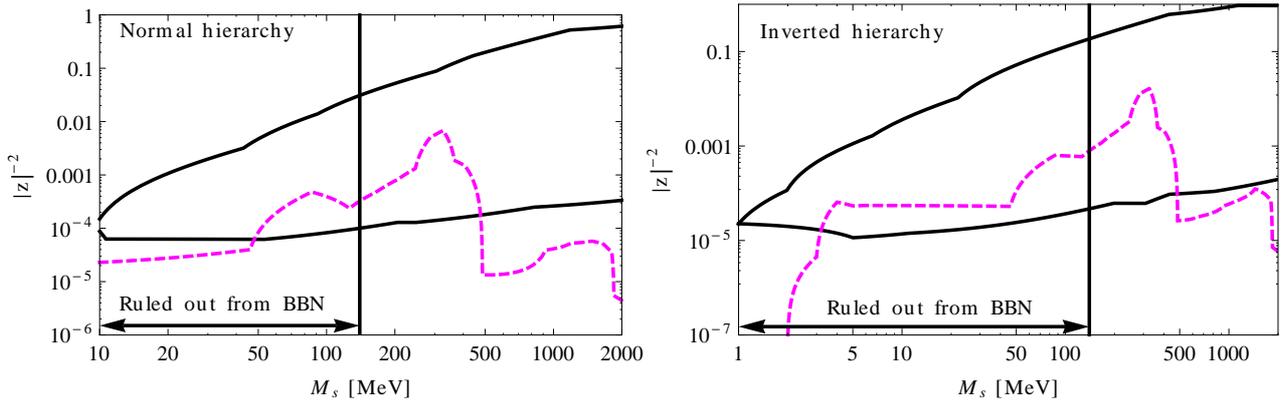
---

[16]`http://sec.bitp.kiev.ua`
[17]`http://virgo.org.ua`

Figure 9: The region of successful baryogenesis in the νMSM compared with the experimental upper bounds on the parameter $|z|$. The vales of M_s and $|z|$, lying inside the black solid lines lead to the production of the observable baryon asymmetry (from [31]). The magenta dashed line marks is the *lower* bound on $|z|^{-2}$ (parameter, called ϵ in [13, 31]) such that for smaller values at least one of the mixing angles ϑ_α^2 is in contradiction with direct experimental searches (for the best-fit values of the PMNS mixing angles and masses). The value of $|z|$ corresponding to the bound is what we refer to as $z_{\max}$ in Sec. 3.4. The region to the left of $M_s = 140\,\mathrm{MeV}$ is ruled out from comparison with primordial nucleosynthesis bounds (Fig. 8).

[7] P. Minkowski, *mu → e gamma at a rate of one out of 1-billion muon decays?*, *Phys. Lett.* **B67** (1977) 421.

[8] P. Ramond, *The family group in grand unified theories*, `hep-ph/9809459`.

[9] R. N. Mohapatra and G. Senjanovic, *Neutrino mass and spontaneous parity nonconservation*, *Phys. Rev. Lett.* **44** (1980) 912.

[10] T. Yanagida, *Horizontal gauge symmetry and masses of neutrinos*, *Prog. Theor. Phys.* **64** (1980) 1103.

[11] A. Atre, T. Han, S. Pascoli and B. Zhang, *The Search for Heavy Majorana Neutrinos*, *JHEP* **05** (2009) 030 [`0901.3589`].

[12] D. Gorbunov and M. Shaposhnikov, *How to find neutral leptons of the numsm?*, *JHEP* **10** (2007) 015 [`arXiv:0705.1729 [hep-ph]`].

[13] M. Shaposhnikov, *The nuMSM, leptonic asymmetries, and properties of singlet fermions*, *JHEP* **08** (2008) 008 [`0804.4542`].

[14] A. D. Dolgov, S. H. Hansen, G. Raffelt and D. V. Semikoz, *Cosmological and astrophysical bounds on a heavy sterile neutrino and the KARMEN anomaly*, *Nucl. Phys.* **B580** (2000) 331–351 [`hep-ph/0002223`].

[15] A. D. Dolgov, S. H. Hansen, G. Raffelt and D. V. Semikoz, *Heavy sterile neutrinos: Bounds from big-bang nucleosynthesis and SN 1987A*, *Nucl. Phys.* **B590** (2000) 562–574 [`hep-ph/0008138`].

[16] A. Boyarsky, O. Ruchayskiy and M. Shaposhnikov, *The role of sterile neutrinos in cosmology and astrophysics*, *Ann. Rev. Nucl. Part. Sci.* **59** (2009) 191 [`0901.0011`].

[17] T. Asaka, S. Eijima and H. Ishida, *Mixing of Active and Sterile Neutrinos*, *JHEP* **1104** (2011) 011 [`1101.1382`].

[18] **DAYA-BAY Collaboration** Collaboration, F. An *et. al.*, *Observation of electron-antineutrino disappearance at Daya Bay*, `1203.1669`.

[19] **RENO collaboration** Collaboration, J. Ahn *et. al.*, *Observation of Reactor Electron Antineutrino Disappearance in the RENO Experiment*, `1204.0626`.

[20] **MINOS** Collaboration, P. Adamson *et. al.*, *Improved search for muon-neutrino to electron-neutrino oscillations in MINOS*, *Phys.Rev.Lett.* **107** (2011) 181802 [`1108.0015`].

[21] **T2K** Collaboration, K. Abe *et. al.*, *Indication of Electron Neutrino Appearance from an Accelerator-produced Off-axis Muon Neutrino Beam*, *Phys.Rev.Lett.* **107** (2011) 041801 [`1106.2822`].

[22] O. Ruchayskiy and A. Ivashko, *Restrictions on the lifetime of sterile neutrinos from primordial nucleosynthesis*, `1202.2841`.

[23] V. Gorkavenko and S. Vilchynskiy, *Some constraints on the Yukawa parameters in the neutrino modification of the Standard Model (nuMSM) and CP-violation*, *Eur.Phys.J.* **C70** (2010) 1091–1098 [`0907.4484`].

[24] World Scientific, *International Conference on the Seesaw Mechanism*, (Singapore), World Scientific, 2005.

[25] J. Schechter and J. Valle, *Neutrino Masses in SU(2) x U(1) Theories*, *Phys.Rev.* **D22** (1980) 2227.

[26] J. Schechter and J. Valle, *Neutrino Decay and Spontaneous Violation of Lepton Number*, *Phys.Rev.* **D25** (1982) 774.

[27] W. Rodejohann and J. Valle, *Symmetrical Parametrizations of the Lepton Mixing Matrix*, *Phys.Rev.* **D84** (2011) 073011 [`1108.3484`].

[28] T. Asaka, S. Blanchet and M. Shaposhnikov, *The numsm, dark matter and neutrino masses*, *Phys. Lett.* **B631** (2005) 151–156 [`hep-ph/0503065`].

[29] T. Asaka and M. Shaposhnikov, *The nuMSM, dark matter and baryon asymmetry of the universe [rapid communication]*, *Phys. Lett. B* **620** (July, 2005) 17–26 [`arXiv:hep-ph/0505013`].

[30] A. Boyarsky, A. Neronov, O. Ruchayskiy and M. Shaposhnikov, *The masses of active neutrinos in the nuMSM from X-ray astronomy*, *JETP Letters* (2006) 133–135 [`hep-ph/0601098`].

[31] L. Canetti and M. Shaposhnikov, *Baryon Asymmetry of the Universe in the NuMSM*, *JCAP* **1009** (2010) 001 [`1006.0133`].

[32] M. Shaposhnikov, *A possible symmetry of the numsm*, *Nucl. Phys.* **B763** (2007) 49–59 [`hep-ph/0605047`].

[33] J. A. Casas and A. Ibarra, *Oscillating neutrinos and mu –¿ e, gamma*, *Nucl. Phys.* **B618** (2001) 171–204 [`hep-ph/0103065`].

[34] G. Bernardi *et. al.*, *SEARCH FOR NEUTRINO DECAY*, *Phys. Lett.* **B166** (1986) 479.

[35] G. Bernardi *et. al.*, *Further limits on heavy neutrino couplings*, *Phys. Lett.* **B203** (1988) 332.

[36] D. Britton, S. Ahmad, D. Bryman, R. Burnbam, E. Clifford *et. al.*, *Measurement of the $\pi^+ \to e^+\nu$ branching ratio*, *Phys.Rev.Lett.* **68** (1992) 3000–3003.

[37] D. Britton, S. Ahmad, D. Bryman, R. Burnham, E. Clifford *et. al.*, *Improved search for massive neutrinos in $\pi^+ \to e^+\nu$ decay*, *Phys.Rev.* **D46** (1992) 885–887.

[38] **NuTeV** Collaboration, A. Vaitaitis *et. al.*, *Search for neutral heavy leptons in a high-energy neutrino beam*, *Phys. Rev. Lett.* **83** (1999) 4943–4946 [`hep-ex/9908011`].

[39] **CHARM** Collaboration, F. Bergsma *et. al.*, *A SEARCH FOR DECAYS OF HEAVY NEUTRINOS IN THE MASS RANGE 0.5-GeV TO 2.8-GeV*, *Phys.Lett.* **B166** (1986) 473.

[40] T. Yamazaki *et. al.*, *Search for heavy neutrinos in kaon decay*, . IN *LEIPZIG 1984, PROCEEDINGS, HIGH ENERGY PHYSICS, VOL. 1*, 262.

[41] R. Hayano, T. Taniguchi, T. Yamanaka, T. Tanimori, R. Enomoto *et. al.*, *HEAVY NEUTRINO SEARCH USING K(mu2) DECAY*, *Phys.Rev.Lett.* **49** (1982) 1305.

[42] D. Bryman and T. Numao, *Search for massive neutrinos in $\pi+ \to \mu + \nu$ decay*, *Phys.Rev.* **D53** (1996) 558–559.

[43] R. Abela, M. Daum, G. Eaton, R. Frosch, B. Jost *et. al.*, *SEARCH FOR AN ADMIXTURE OF HEAVY NEUTRINO IN PION DECAY*, *Phys.Lett.* **B105** (1981) 263–266.

[44] M. Daum, B. Jost, R. Marshall, R. Minehart, W. Stephens *et. al.*, *SEARCH FOR ADMIXTURES OF MASSIVE NEUTRINOS IN THE DECAY pi+ —¿ mu+ neutrino*, *Phys.Rev.* **D36** (1987) 2624.

[45] **PIENU Collaboration** Collaboration, M. Aoki *et. al.*, *Search for Massive Neutrinos in the Decay $\pi \to e\nu$*, *Phys.Rev.* **D84** (2011) 052002 [`1106.4055`].

[46] **DELPHI** Collaboration, P. Abreu *et. al.*, *Search for neutral heavy leptons produced in Z decays*, *Z.Phys.* **C74** (1997) 57–71.

[47] M. Blennow, E. Fernandez-Martinez, J. Lopez-Pavon and J. Menendez, *Neutrinoless double beta decay in seesaw models*, *JHEP* **1007** (2010) 096 [`1005.3240`].

[48] F. Bezrukov, *numsm predictions for neutrinoless double beta decay*, *Phys. Rev.* **D72** (2005) 071303 [`hep-ph/0505247`].

[49] R. E. Shrock, *New Tests For, and Bounds On, Neutrino Masses and Lepton Mixing*, *Phys. Lett.* **B96** (1980) 159.

[50] R. E. Shrock, *General Theory of Weak Leptonic and Semileptonic Decays. 1. Leptonic Pseudoscalar Meson Decays, with Associated Tests For, and Bounds on, Neutrino Masses and Lepton Mixing*, *Phys.Rev.* **D24** (1981) 1232.

[51] R. E. Shrock, *General Theory of Weak Processes Involving Neutrinos. 2. Pure Leptonic Decays*, *Phys.Rev.* **D24** (1981) 1275.

[52] R. E. Shrock, *PURE LEPTONIC DECAYS WITH MASSIVE NEUTRINOS AND ARBITRARY LORENTZ STRUCTURE*, *Phys.Lett.* **B112** (1982) 382.

[53] A. Kusenko, S. Pascoli and D. Semikoz, *New bounds on MeV sterile neutrinos based on the accelerator and Super-Kamiokande results*, *JHEP* **0511** (2005) 028 [hep-ph/0405198].

[54] **NOMAD** Collaboration, P. Astier *et. al.*, *Search for heavy neutrinos mixing with tau neutrinos*, *Phys. Lett.* **B506** (2001) 27–38 [hep-ex/0101041].

[55] J.-M. Levy, *Doctoral thesis, university of paris (1986)*, .

[56] **LBNE Collaboration** Collaboration, T. Akiri *et. al.*, *The 2010 Interim Report of the Long-Baseline Neutrino Experiment Collaboration Physics Working Groups*, 1110.6249.

[57] K. Abazajian, M. Acero, S. Agarwalla, A. Aguilar-Arevalo, C. Albright *et. al.*, *Light Sterile Neutrinos: A White Paper*, 1204.5379.

[58] A. Shaykhiev, Y. Kudenko and A. Khotyantsev, *Searches for heavy neutrinos in the decays of positively charged kaons*, *Phys.Atom.Nucl.* **74** (2011) 788–793.

[59] A. Kusenko, *Sterile neutrinos, dark matter, and the pulsar velocities in models with a higgs singlet*, *Phys. Rev. Lett.* **97** (2006) 241301 [hep-ph/0609081].

[60] I. M. Shoemaker, K. Petraki and A. Kusenko, *Collider signatures of sterile neutrinos in models with a gauge-singlet Higgs*, *JHEP* **1009** (2010) 060 [1006.5458].

[61] J. Dunkley, R. Hlozek, J. Sievers, V. Acquaviva, P. Ade *et. al.*, *The Atacama Cosmology Telescope: Cosmological Parameters from the 2008 Power Spectra*, *Astrophys.J.* **739** (2011) 52 [1009.0866].

[62] E. Aver, K. A. Olive and E. D. Skillman, *An MCMC determination of the primordial helium abundance*, 1112.3713.

[63] Y. Izotov and T. Thuan, *The primordial abundance of 4He: evidence for non-standard big bang nucleosynthesis*, *Astrophys.J.* **710** (2010) L67–L71 [1001.4440].

[64] G. M. Fuller, C. T. Kishimoto and A. Kusenko, *Heavy sterile neutrinos, entropy and relativistic energy production, and the relic neutrino background*, 1110.6479.

[65] E. K. Akhmedov, V. A. Rubakov and A. Y. Smirnov, *Baryogenesis via neutrino oscillations*, *Phys. Rev. Lett.* **81** (1998) 1359–1362 [hep-ph/9803255].

[66] X.-d. Shi and G. M. Fuller, *A new dark matter candidate: Non-thermal sterile neutrinos*, *Phys. Rev. Lett.* **82** (1999) 2832–2835 [`astro-ph/9810076`].

[67] M. Laine and M. Shaposhnikov, *Sterile neutrino dark matter as a consequence of νMSM-induced lepton asymmetry*, *JCAP* **6** (June, 2008) 31–+ [`arXiv:0804.4543`].

[68] G. M. Fuller, A. Kusenko and K. Petraki, *Eosphoric sterile neutrinos, supernovae, and the galactic positrons*, *Phys. Lett.* **B670** (2009) 281–284 [`0806.4273`].

[69] G. Gelmini, S. Palomares-Ruiz and S. Pascoli, *Low reheating temperature and the visible sterile neutrino*, *Phys. Rev. Lett.* **93** (2004) 081302 [`astro-ph/0403323`].

[70] G. Gelmini, E. Osoba, S. Palomares-Ruiz and S. Pascoli, *MeV sterile neutrinos in low reheating temperature cosmological scenarios*, *JCAP* **0810** (2008) 029 [`0803.2735`].

A Sterile neutrino lifetime

For any phenomenologically interesting mass of the sterile neutrino it can decay to three neutrinos $N \to \nu\bar{\nu}\nu$ and it results in contribution

$$B_{\nu\nu\nu}^e = B_{\nu\nu\nu}^\mu = B_{\nu\nu\nu}^\tau = 1 \tag{38}$$

to the total sum in Eq. (2) over decay products X.

If $M_s > 2M_e \approx 1.0$ MeV, then a new decay channel appears: $N \to e^+ e^- \nu$. It corresponds to

$$
\begin{aligned}
B_{ee\nu}^\alpha = {} & (\frac{1}{4} \pm \sin^2\theta_W + 2\sin^4\theta_W)\Bigg[\left(1 - 14S_e^2 - 2S_e^4 - 12S_e^6\right)\sqrt{1 - 4S_e^2} \\
& + 12S_e^4 \left(S_e^4 - 1\right) \ln\left(\frac{1 - 3S_e^2 - (1 - S_e^2)\sqrt{1 - 4S_e^2}}{S_e^2(1 + \sqrt{1 - 4S_e^2})}\right)\Bigg] \\
& + 2\sin^2\theta_W (2\sin^2\theta_W \pm 1)\Bigg[S_e^2(2 + 10S_e^2 - 12S_e^4)\sqrt{1 - 4S_e^2} \\
& + 6S_e^4(1 - 2S_e^2 + 2S_e^4)\ln\left(\frac{1 - 3S_e^2 - (1 - S_e^2)\sqrt{1 - 4S_e^2}}{S_e^2(1 + \sqrt{1 - 4S_e^2})}\right)\Bigg] ,
\end{aligned}
$$

where $S_X = M_X/M_s$, θ_W is the Weinberg angle, and sign "+" corresponds to $\alpha = e$ while "-" in the other case. For $S_\mu < \frac{1}{2}$ we should add up to a sum terms $B_{\mu\mu\nu}^\alpha$ that can be obtained from $B_{ee\nu}^\alpha$ if one changes $S_e \to S_\mu$ and if sign "+" corresponds to $\alpha = \mu$, "-" - to $\alpha = e, \tau$.

Other B-coefficients are

$$B_{e\mu\nu}^{e,\mu} = 1 - 8S_\mu^2 + 8S_\mu^6 - S_\mu^8 - 24S_\mu^4 \ln S_\mu, \quad B_{e\mu}^\tau = 0, \quad (S_\mu + S_e < 1) , \tag{39}$$

$$B_{\pi\nu}^\alpha = 6\pi^2 \frac{f_\pi^2}{M_s^2}(1 - S_\pi^2)^2, \quad (S_\pi < 1, \ M_\pi \approx 140 \text{ MeV}, \ f_\pi \approx 130 \text{ MeV}) , \tag{40}$$

$$B_{\eta\nu}^{\alpha} = 6\pi^2 \frac{f_\eta^2}{M_s^2}(1 - S_\eta^2)^2, \quad (S_\eta < 1, \ M_\eta \approx 550 \,\mathrm{MeV}, \ f_\eta \approx 155 \,\mathrm{MeV}), \tag{41}$$

$$B_{\pi e}^{e} = 12\pi^2 \frac{f_\pi^2}{M_s^2}V_{ud}^2\left((1-S_e^2)^2 - S_\pi^2(1+S_e^2)\right)\sqrt{(1 - (S_\pi - S_e)^2)(1 - (S_\pi + S_e)^2)}, \quad (S_e + S_\pi < 1), \tag{42}$$

$$B_{\pi\mu}^{\mu} = 12\pi^2 \frac{f_\pi^2}{M_s^2}V_{ud}^2\left((1-S_\mu^2)^2 - S_\pi^2(1+S_\mu^2)\right)\sqrt{(1 - (S_\pi - S_\mu)^2)(1 - (S_\pi + S_\mu)^2)}, \quad (S_\mu + S_\pi < 1). \tag{43}$$

In the last expression quantity $V_{ud} \approx 0.97$ is the element of the Cabibbo-Kobayashi-Maskawa (CKM) quark matrix. Expression for B_{Ke}^e, that is non-zero for mass range $S_e + S_K < 1$ ($M_K \approx 495 \,\mathrm{MeV}$), can be derived from $B_{\pi e}^e$ by simultaneous change $S_\pi \to S_K, V_{ud} \to V_{us} \approx 0.23$, $f_\pi \to f_K \approx 160 \,\mathrm{MeV}$. Moreover, if we change in the resulting expression S_e by S_μ, we get $B_{K\mu}^\mu$ (for $S_\mu + S_K < 1$). What concerns B-coefficients with $\alpha = \tau$ and $X = (\pi e, \ \pi\mu, \ Ke, \ K\mu)$, they are all zero. For masses of sterile neutrino, that are larger than the mass of the ρ-meson $M_\rho \approx 780 \,\mathrm{MeV}$, other B_X appear. We do not list list them in the present paper, however they can be read from [12].

B PMNS parametrization

In Section 3 we use the standard definition of the PMNS matrix (cf. e.g. [1]):

$$V = \begin{pmatrix} 1 & 0 & 0 \\ 0 & c_{23} & s_{23} \\ 0 & -s_{23} & c_{23} \end{pmatrix} \begin{pmatrix} c_{13} & 0 & s_{13} \\ 0 & e^{i\phi} & 0 \\ -s_{13} & 0 & c_{13} \end{pmatrix} \begin{pmatrix} c_{12} & s_{12} & 0 \\ -s_{12} & c_{12} & 0 \\ 0 & 0 & 1 \end{pmatrix}$$

$$= \begin{pmatrix} c_{12}c_{13} & c_{13}s_{12} & s_{13} \\ -c_{23}s_{12}e^{i\phi} - c_{12}s_{13}s_{23} & c_{12}c_{23}e^{i\phi} - s_{12}s_{13}s_{23} & c_{13}s_{23} \\ s_{23}s_{12}e^{i\phi} - c_{12}c_{23}s_{13} & -c_{12}s_{23}e^{i\phi} - c_{23}s_{12}s_{13} & c_{13}c_{23} \end{pmatrix}. \tag{44}$$

where $c_{ij} = \cos\theta_{ij}$, and $s_{ij} = \sin\theta_{ij}$. The active neutrino mixing matrix is given by expression (5).

C Ratio of sterile neutrino mixing angles for $|z| \sim 1$

As the expressions (12) and (20) show, the mixing angles have two terms: one is proportional to $|z|^2$ and another to $|z|^{-2}$ (recall that $|z| \geq 1$). It was shown in Sec. 3.3 that for inverted hierarchy the $|z|^2$-term can be zero for ϑ_μ^2 and ϑ_τ^2, while the $|z|^{-2}$ term in general stays finite.

For a given value of $|z|$, the $|z|^{-2}$-term is bounded from above. According to (12) and (20), its maximum is realized simultaneously with the maximal value of

$$L_\alpha^{NH} = |V_{\alpha 3} + ie^{i\xi}\sqrt{\frac{m_2}{m_3}}V_{\alpha 2}|^2 \tag{45}$$

in the normal hierarchy, and

$$L_\alpha^{IH} = |V_{\alpha 1} + ie^{i(\xi - \zeta)}\sqrt{\frac{m_2}{m_1}}V_{\alpha 2}|^2 \tag{46}$$

in the inverted hierarchy.

Analysis, similar to that of the Sections 3.2–3.3 shows that

$$L_e^{NH} \leq 0.2, \quad L_\mu^{NH} \leq 1.1, \quad L_\tau^{NH} \leq 1.1, \quad L_e^{IH} \leq 1.96, \quad L_\mu^{IH} \leq 1.3, \quad L_\tau^{IH} \leq 1.3 . \tag{47}$$

These bounds allow to estimate the contribution of the $|z|^{-2}$-terms to the whole sum of the squared mixing angles

$$\sum_\alpha \vartheta_\alpha^2 = \frac{m_1 + m_2 + m_3}{4M_s} \left(|z| + \frac{1}{|z|} \right) . \tag{48}$$

The ratio of (45)–(46) to (48) gives

$$R_\alpha^{NH} = \frac{L_\alpha^{NH}}{(1 + \frac{m_2}{m_3})} \frac{1}{|z|^4 + 1}, \quad R_\alpha^{IH} = \frac{L_\alpha^{IH}}{(1 + \frac{m_2}{m_1})} \frac{1}{|z|^4 + 1} . \tag{49}$$

For $z \sim 1$ it can become of order unity. However, we restrict ourselves to the sufficiently large values $z \gtrsim 10$, that are consistent with the upper bound, indicated by the experiments (see Fig.9)

$$R_e^{NH} \lesssim 2 \times 10^{-5}, \quad R_{\mu,\tau}^{NH} \lesssim 10^{-4}, \quad R_e^{IH} \lesssim 10^{-4}, \quad R_{\mu,\tau}^{IH} \lesssim 5 \times 10^{-5} . \tag{50}$$

Comparison these results with the *lower* bounds (Table 2) we see that z^{-1} terms are unimportant for the for all mixing angles in NH and ϑ_e in IH. What concerns the remaining angles ϑ_μ and ϑ_τ in IH, they can be substantially modified by account of z^{-1}-terms, but anyway each of them can become small enough, compared to the other angles, as explained in next section. As a corollary, analysis and results of Secs. 3.2,3.3 do not change significantly for large enough values of z.